Journal of Water Process Engineering 37 (2020) 101501

Contents lists available at ScienceDirect

Journal of Water Process Engineering

journal homepage: www.elsevier.com/locate/jwpe

Photocatalytic ozonation for sea water decontamination

Chi Chung Tsoi[a], Xiaowen Huang[b], Polly H.M. Leung[c], Ning Wang[d], Weixing Yu[e], Yanwei Jia[f], Zhaohui Li[g], Xuming Zhang[a,*]

[a] Department of Applied Physics, The Hong Kong Polytechnic University, Hong Kong
[b] State Key Laboratory of Biobased Material and Green Papermaking, Department of Bioengineering, Qilu University of Technology (Shandong Academy of Sciences), China
[c] Department of Health Technology and Informatics, The Hong Kong Polytechnic University, Hong Kong
[d] National Engineering Laboratory for Fiber Optic Sensing Technology, Wuhan University of Technology, Wuhan, China
[e] Key Laboratory of Spectral Imaging Technology, Xi'an Institute of Optics and Precision Mechanics, Chinese Academy of Sciences, Xi'an, China
[f] State Key Laboratory of Analog and Mixed Signal VLSI, Institute of Microelectronics, University of Macau, Macau, China
[g] School of Electronics and Information Engineering, Sun Yat-Sen University, Guangzhou, China

ARTICLE INFO

Keywords:
Photocatalysis
Ozonation
Sea water
Decontamination
Wastewater treatment

ABSTRACT

Polluted sea water is a common problem in coastal cities, but its decontamination remains a big challenge due to the existence of salt ions, which may invalidate many prevailing treatment methods originally developed for waste fresh water. This work presents the first attempt to decontaminate the polluted sea water by synergizing two separate processes: photocatalysis and ozonation. For low cost and human safety, the ozone concentration is kept to be < 60 ppm in the pumping gas (0.026 ppm in solution). Mechanism studies and experimental comparisons show that the photocatalysis, the ozonation and the photocatalytic ozonation (PCO) all have lower efficiencies in sea water than that in fresh water, and the PCO is always more efficient than only the photocatalysis or only the ozonation. More specifically, the PCO has a reaction rate constant about 23 times higher than only the ozonation. In addition, the sea water shows a positive synergistic effect of photocatalysis and ozonation and reaches the maximum when the pumping gas has an ozone concentration of 50 ppm in gas. In contrast, the fresh water shows a negative synergistic effect. Mechanism study using experiments infers that the dissolved ozone can enhance and stabilize the photocurrent by rapidly scavenging the photoelectrons. This work may pave the way to practical applications of sea water decontamination with high efficiency and low cost.

1. Introduction

Waste water has long been a big problem of modern society [1]. Most of the waste water results from the use of fresh water (e.g., bathing, washing machine) and thus the major effort of waste water treatment has been made to the polluted fresh water. To save the precious fresh water resource, many coastal cities (e.g., Hong Kong) choose to use sea water for routine tasks (e.g., toilet flushing, pavement washing), and thus produce huge amount of polluted sea water. Due to the existence of salt ions, most prevailing waste water treatment methods (e.g., chemical method, bacteria growth) that are highly efficient for polluted fresh water do not work for the polluted sea water [2].

Other advanced oxidation processes such as photocatalysis and ozonation have been attempted to decontaminate the waste sea water [1,3,4]. Nevertheless, the photocatalysis [5–9] usually has low efficiency in sea water. This is because both inorganic cations (i.e., Ca^{2+}, Cu^{2+}, Mg^{2+}, Fe^{2+}, Zn^{2+}, Al^{3+}) and inorganic anions (i.e., Cl^-, ClO_3^-, IO_4^-, PO_4^{3-}) adversely affect the photocatalytic water treatment [10–14]. It is found that Cu^{2+}, Fe^{2+}, Al^{3+}, Cl^-, PO_4^{3-} may decrease oxidization reaction rates while Ca^{2+}, Mg^{2+}, Zn^{2+} often have negligible effect. Besides, the Cl^- accounts for the inhibitory effect on TiO_2 photocatalysis through a preferential adsorption displacement mechanism over the surface bound OH^- ions. This reduces the number of OH^- ions available on the TiO_2 surface, and the substituted Cl^- also increases the recombination of electron-hole pairs.

Similarly, ozone has been applied to decontaminate the waste sea water but has shown reduced degradation performance [15,16], again due to the salt ions. Photocatalytic ozonation (PCO) is a combination of both the photocatalytic process and the ozonation process at the same

* Corresponding author.
E-mail addresses: terry.cc.tsoi@connect.polyu.hk (C.C. Tsoi), huangxiaowen2013@gmail.com (X. Huang), polly.hm.leung@polyu.edu.hk (P.H.M. Leung), ningwang23@whut.edu.cn (N. Wang), yuwx@opt.ac.cn (W. Yu), yanweijia@um.edu.mo (Y. Jia), lzhh88@mail.sysu.edu.cn (Z. Li), apzhang@polyu.edu.hk (X. Zhang).

https://doi.org/10.1016/j.jwpe.2020.101501
Received 24 May 2020; Received in revised form 2 July 2020; Accepted 6 July 2020

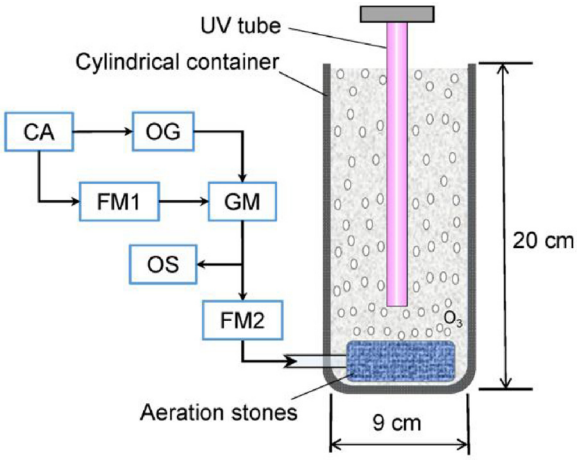

Fig. 1. Schematic diagram of the experimental setup. The cylindrical reactor contains the water sample and has a UV tube inserted at the center as the light source. The bottom of the reactor has aeration stones for dispersing the pumped gas into bubbles. The concentration of ozone is controlled by mixing the compressed air with the ozone from an ozone generator. CA: compressed air source; OG: ozonation generator; FM1: flow meter 1; GM: gas mixer; OS: ozone sensor; FM2: flow meter 2.

time. It is found very promising for the treatment of waste fresh water, and there is even a synergistic effect of photocatalysis and ozonation [17]. Nevertheless, little work has been done to explore the PCO for the waste sea water. This paper aims to fill this gap by conducting mechanism studies and experimental investigations of the PCO in sea water. We will try to find the optimal conditions of the PCO, to examine the synergistic effect and to study the influence of salinity.

2. Materials and methods

2.1. Experimental setup

Decontamination experiment is carried out using a reactor system as shown in Fig. 1. The UV reactor consists of a cylindrical container (height 20 cm and inner diameter 9 cm), a UV light source and an ozone supply system. The cylindrical container is a glass bottle which filled with the water sample. The UV light source is a medium pressure Hg tube (25 W with 8 W (94 μW/cm^2) in the UV-C spectrum, from Cnlight Ltd). It is inserted along the central line of the container to irradiate the water sample. The ozone supply system utilizes compressor air as the gas source. Part of the compressed air (CA) goes through an ozone generator (OG, from YEK High-Tech Ltd.) to generate ozone gas by electric discharge. The other part of compressed air is monitored by a flow meter (FM1) and is then used to dilute the ozone gas via a gas mixer (GM). An ozone sensor (OS, from Bosean) is used to monitor the ozone concentration and another flow meter (FM2) is used to measure the flow rate of mixed ozone gas. The ozone concentration can be controlled by adjusting the flow rate of the diluting compressed air. Finally, the ozone gas is pumped into the bottom of the cylindrical container. Two aeration stones (length 27 mm and diameter 12 mm) are used to disperse the ozone gas into small bubbles. A hole is drilled at the side surface of the bottle near the bottom, through which the tube injects the ozone gas into the aeration stones. This improves the dissolution of ozone into water and helps stir the water sample when the bubbles move up.

In the decontamination experiments, if only the ozonation effect is tested, the photocatalyst and the UV tube are not placed in the cylindrical container. For the photocatalysis and/or the UV effect, the photocatalyst and/or the UV tube will be used correspondingly. After the degradation process, the water sample is measured by a UV–vis spectrometer (UV-2550, spectral range 250–900 nm, from Shimadzu). The 665-nm absorptance of the treated solution is ratioed to that of the original solution to represent the concentration of methylene blue (MB). Then, the decontamination rate can be calculated.

2.2. Materials

To indicate the degradation, the model chemical utilizes the dye solution of MB with the concentration of 3×10^{-5} M. The sea water sample is 35 wt% (non-purified, raw) sea salt with deionized (DI) water, corresponding to the NaCl concentration of 0.6 M. The photocatalytic material is P25 TiO_2 nanopowder (Aeroxide, Sigma Aldrich) with the primary particle size of 21 nm. The TiO_2 solution has the concentration of 1 g·L^{-1}. After the decontamination, the nanopowders can be removed by centrifugation.

2.3. Experimental procedures

The experimental studies of this work consist of several tests: solubility of ozone, comparison of ozonation and photocatalysis, synergistic effect of PCO, and influences of salt concentration on the PCO. Here we elaborate the details of experimental procedures.

To test the solubility of ozone in sea water and DI water, standard starch-iodide method is used to measure the ozone concentration. Previous study reported a detection limit down to 75 ppbw, which is equivalent to 75 μg L^{-1}. In this work, the basic water samples are deionized water (DIW, resistivity 18.2 MΩ cm) and sea water. Different concentrations of ozone are pumped into the solutions in the reactor system. Overdosed potassium iodide (KI) is added into the solution to obtain iodine. Then, starch is added into the water sample, whose color would be changed from colorless to dark-blue in the presence of dissolved ozone. The color of the dark-blue solution is measured by the UV–vis spectrometer. Other tests for the iodine concentration in water are also conducted for calibration. Different concentrations of iodine are added into 5% ethanol solution with starch. And the color of dark blue is measured by the UV–vis spectrometer as well.

To test the ozonation effect in different concentrations of ozone [17], the sea water with 30 μM MB is blown by different concentrations of ozone gas. And the color change is measured by the UV–vis spectrometer too. Similarly, the PCO effect is tested with different concentrations of ozone; however, TiO_2 nanoparticle (concentration 1 g·L^{-1}) is added into the solution and the UV tube is used to provide the ultraviolet C (UV-C) irradiation during the reaction. In addition, the photocatalytic degradation using the 30 μM MB solution is carried out as the reference. To find out the synergistic effect of the photocatalysis and the ozonation, the degradation efficiencies of the photocatalysis, the PCO and the ozonation are compared.

To study the influence of salt concentration, the PCO experiments utilize 25 %, 50 % and 75 % sea water solutions with 30 μM MB. Here the percentages of 25 %, 50 % and 75 % represent the concentration relative to the standard sea water. The procedures are similar to those of the PCO tests using different concentrations of ozone, except that here the concentration of ozone is fixed.

3. Mechanisms

3.1. Mechanisms of photocatalysis, ozonation and PCO in fresh water and sea water

For proper design of experiments and appropriate interpretation of test results in this work, the reaction mechanisms that underlie the photocatalysis, the ozonation and the PCO should be investigated. Many articles have reported detailed studies [18–27]. Here we will summarize those directly related to our work. Fig. 2(a) depicts the mechanism of photo-excited electrons and holes pair when the TiO_2 particle is irradiated by the photons with the energy ≥ 3.2 eV [28]. On the TiO_2 surface, the electrons and holes can be captured by the ions

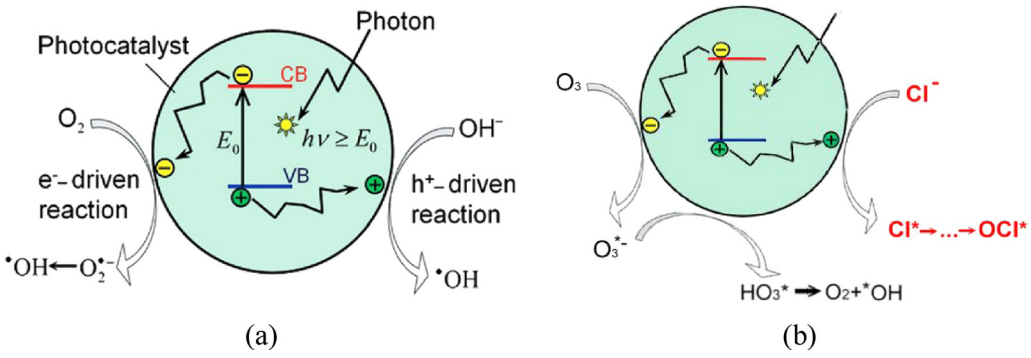

Fig. 2. Mechanisms of the semiconductor photocatalysis in fresh water and the photocatalytic ozonation in sea water; (a) In the photocatalysis of fresh water, the photo-excited electrons and holes react with dissolved O_2 and OH^- to generate free *OH radicals, which has high oxidation power to oxidized most organic pollutants; [40] (b) In the photocatalytic ozonation of sea water, the electrons are captured by O_3 to generate *OH, and the holes are scavenged by Cl^- ions to generate OCl* radicals.

and other chemical species in the water sample. In the fresh water, the major compounds are H^+, OH^- and dissolved O_2. In the sea water, there are abundant Cl^- ions. For instance, the concentration of Cl- is 0.6 M in 3.5 wt% sea water. Therefore, the reaction pathways become different.

For the photocatalysis in the fresh water, the holes can directly oxidize the organic pollutants or combine with OH^- to form *OH radicals, which are highly oxidative; and the electrons can be scavenged by the adsorbed O_2 molecules, which eventually form *OH radicals for oxidation of the organic pollutants [18–20]. However, in the sea water, the photocatalytic reactions are very different, as illustrated in Fig. 2(b). In this case, the direct hole oxidation is prohibited. Instead, the holes are scavenged by the abundant Cl^- ions to convert into the Cl* radicals and the OCl* radicals, which are all oxidative [13,29–32]. Now we can see that the major oxidative species are the Cl* radicals in the sea water, as compared to the *OH radicals in the fresh water. Since Cl* has weaker oxidation power than *OH, the sea water has a weaker photocatalytic activity than the fresh water [33–39]. For easy discussion, the oxidation powers of some common agents are listed in Table 1. For instance, the hydroxyl radical *OH has the redox potential of 2.86 V with respect to standard hydrogen electrode (SHE), just slightly lower than that of fluorine atom (2.87 V vs. SHE).

The ozonation processes are also different in fresh water and sea water. In fresh water, the dissolved ozone molecules can directly oxidize the organic molecules, or combine with OH^- ions to form *OH radicals [41,42]. In sea water, the ozone molecules can still contribute to the direction oxidizing reaction. Nevertheless, the abundance of salt ions like Cl^- makes it more probably go through indirect reactions to form ClO^- and ClO_3^- ions. [43–45] In the sea water, the oxidizing species are mainly ClO^-, which are different from *OH radicals in the fresh water. Since the oxidizing power of ClO^- (potential 1.49 V vs. SHE, see Table 1) is weaker than that of *OH (potential 2.86 V vs. SHE), it is expected that the ozonation effect in sea water is weaker than that in fresh water.

Here we present more details of the mechanisms of PCO in fresh water and sea water. In fresh water, the ozonation in the presence of UV-irradiated TiO_2 can produce OH ˙radicals by forming an ozonide radical (O3*⁻, see Fig. 2(b)) [46,47], which can go further to form the *OH radicals. The reactions are as below.

$$O_3 + e- \rightarrow O_3^* \quad (1)$$

$$O_3^{*-} + H+ \rightarrow HO_3^* \quad (2)$$

$$HO_3^* \rightarrow O_2 + {}^*OH \quad (3)$$

In sea water, the Cl^- ions can react with the already-generated oxidizing radicals (e.g., HO_3*, *OH) by possible reactions like (see Fig. 2(b))

$$HO_3^* + Cl^- \rightarrow Cl^* + OH^- + O_2 \quad (4)$$

$$^*OH + Cl^- \rightarrow OCl^{*-} + H_2O \quad (5)$$

$$OCl^{*-} + H^+ \rightarrow HOCl \quad (6)$$

$$^*OH + ClO_3^- \rightarrow OH^- + {}^*ClO_3 \quad (7)$$

Again, the resulted ions Cl*, OCl^{*-} and $*ClO_3$ have weaker oxidizing powers. Therefore, the sea water has a weaker PCO effect than the fresh water.

Based on the above discussions of the mechanisms, we can summarize that: (i) the sea water has always weaker oxidizing effect than the fresh water in all the processes of the photocatalysis, the ozonation and the PCO, this is due to the reaction of salt ions (like Cl^-) with the highly oxidative radicals (e.g., *OH) to generate relatively weak radicals (like OCl*, $*ClO_3$); (ii) the PCO has faster oxidation rate than only the photocatalysis or only the ozonation due to the combined effect of the direction ozonation and the rapid scavenging of photo-excited electrons. However, the study of mechanisms cannot tell whether the photocatalysis and the ozonation have a synergistic effect (i.e., the PCO effect is higher than the summation of the photocatalytic effect and the ozonation). This needs experimental studies.

Table 1
Redox potential of oxidizing agents with respect to standard hydrogen electrode (SHE) [43].

Species	Potential (V vs. SHE)
Fluorine atom (F)	2.87
Hydroxyl radical (*OH)	2.86
Oxygen atom (O)	2.42
Ozone molecule (O_3)	2.07
Hydrogen peroxide (H_2O_2)	1.78
Hypochlorous acid (HOCl)	1.49
Chlorine atom (Cl)	1.36
Chlorine dioxide (ClO_2)	1.27
Oxygen molecule (O_2)	1.23
Hydrogen atom (H)	0.00

3.2. Experimental proof of rapid scavenging of photo-excited electrons by ozone

As stated above, the dissolved ozone is beneficial to the photocatalysis by the rapid scavenging of photo-excited electrons. This is an important effect. To prove it, we can compare the photocurrents of UV-irradiated TiO_2 without ozone (i.e., only the photocatalysis) and with ozone (i.e., the PCO). The experimental results are showed in Fig. 3. Photocatalysis starts at 1 min with the turn-on of UV light and the continuous pumping of air, the photocurrent density raises from -0.033 mA/cm^2 (dark current) to 0.47 mA/cm^2 (peak at 2.5 min) and gradually drops to 0.42 mA/cm^2 (at 8 min). The reduction of current may be due to the increased electron-hole recombination on the TiO_2 surface. From 8 min, the ozone gas replaces the air to be pumped into the solution, the photocurrent density starts to increase and then becomes stable at 0.61 mA/cm^2 (after 37 min). The replacement of air by ozone results in two results: (1) The photocurrent is increased by ~50 %; (2)

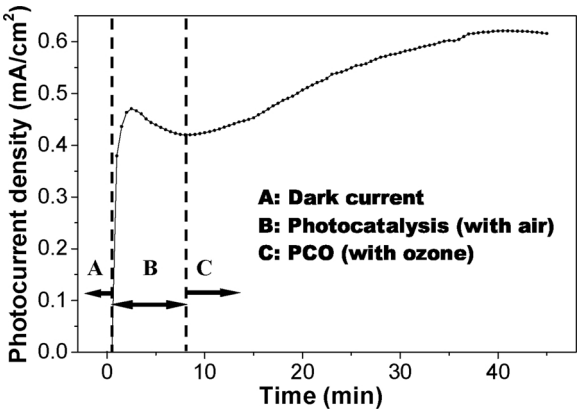

Fig. 3. Proof of the rapid scavenging of photo-excited electrons by the dissolved ozone through comparing the photocurrent densities of the photocatalysis (pumped with air) and the PCO (pumped with ozone). Photocurrent of photocatalysis peaks at 0.47 mA/cm^2 (at 2.5 min) and drops gradually with time. In contrast, photocurrent of PCO peaks at 0.61 mA/cm^2 (after 37 min) and is then stable. The experimental observations show that the presence of ozone has the benefits: (1) increasing the photocurrent by 50 %; and (2) suppressing the electron/hole recombination, proving that the dissolved ozone can rapidly move away the photoelectrons from the TiO_2 surface.

the photocurrent of photocatalysis (i.e., using air) drops gradually while the photocurrent of PCO (i.e., using ozone) is very stable. These can be attributed to the effect that the dissolved ozone can rapidly scavenge the photo-generated electrons from the TiO_2 surface, increasing the photocurrent and suppressing the electron/hole recombination.

4. Results and discussion

4.1. Solubility of ozone in fresh water and sea water

Since the PCO combines the photocatalytic process and the ozonation process at the same time, the solubility of ozone in the solution would directly affect the performance of the organic degradation. Therefore, the solubility is first examined in this work.

In theory, Henry's law is the base for the study of gas solubility. It states that the amount of dissolved gas is proportional to its partial pressure in the gas phase. The proportionality factor is called the Henry's law constant H (i.e., the solubility), which is the ratio of the aqueous phase concentration ca to its gas phase concentration c_g as given by $H = c_a/c_g$. For an ideal gas, the conversion can be transferred as $H = H^{cp} \times RT$, where $H^{cp} = c_a/p$, p is the partial pressure of that matter in the gas phase under equilibrium conditions, R is the gas constant and T is the temperature (in K). Sometimes, this dimensionless constant is also called the "water-air partitioning coefficient" KWA. It is closely related to the slightly different definition of the "Ostwald coefficient" [48].

We have collected the reported experimental data of ozone solubility in fresh water as summarized in Fig. 4, which plots the dimensionless Henry's law constant H as a function of the temperature T [49–52]. It covers the temperature range from 0 to 45 °C. In Fig. 3, the Henry's law constant can be fit by $H = 3.90 \times 10^4 \exp(-0.041T)$. Therefore, the ozone concentrations in fresh water by pumping the 50-ppm gas phase ozone would be 20.4 μg·L^{-1} and 16.6 μg·L^{-1} at 25 °C and 30°C, respectively.

In sea water, the solubility is even lower. It depends considerably on the concentration of salt. The ozone solubility in the aqueous solutions of NaCl, KCl, Na_2SO_4, $MgSO_4$ and $Ca(NO_3)_2$ were measured at 25 °C. At each concentration, three to five experiments were carried out; the mean values of the Henry's law constant are listed in Table 2. The solubility of solutions is generally lower than that of DI water. For

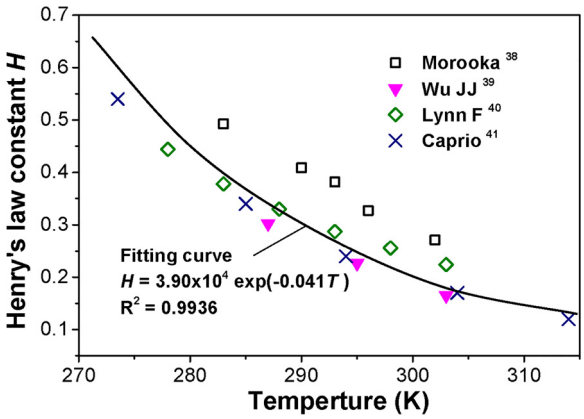

Fig. 4. Solubility of ozone in fresh water (i.e., DI water). The data points are collected from literature and are plotted as dimensionless Henry's law constant H versus temperature T. The increase of temperature leads to a reduction of Henry's law constant and consequently a lower ozone solubility in fresh water.

Table 2
Dimensionless Henry's law constant of ozone in fresh water and salt solutions (with 0.5 M concentration) at 25 °C. The standard deviation results from five repeated tests.

DI water	NaCl	KCl	Na_2SO_4	$MgSO_4$	$Ca(NO_3)_2$
0.268 ± 0.013	0.256 ± 0.005	0.261 ± 0.012	0.162 ± 0.009	0.174 ± 0.012	0.211 ± 0.014

instance, the dimensionless Henry's constant is measured to be $H = 0.267$ in the DI water, but it is only 0.160 for the 0.5-M Na_2SO_4 solution. Nevertheless, it has $H = 0.256$ for the 0.5 M NaCl solution, only slightly lower than that for the DI water ($H = 0.267$). This suggests that the solubility of ozone is similar in the fresh water and the 3.5 wt% sea water (i.e., 0.6 M NaCl).

As discussed above, the dissolved ozone in sea water reacts with the ions and radicals and are then converted to other species. The ozone conversion is strongly affected by the Cl^- concentration. Here the ozone conversion is defined as the ratio of the amount of converted ozone to the amount of initially dissolved ozone. Based on the study of Sotelo in 1989 [53], an increase of Cl^- concentration leads to an increase of the ozone conversion at a given time. It is read from Sotelo's data curves that at the time of 3 ms, the ozone conversion is 55 %, 64 %, 83 % and > 95 % for the NaCl solutions of 0 M (i.e., DI water), 0.05 M, 0.1 M and 0.5 M, respectively. We can see that seawater can quickly absorb almost all ozone as compared to only 55 % of the DI water. It implies a better usage of dissolved ozone in the seawater ozonation than in the freshwater ozonation. This is one of the merits of seawater ozonation.

4.2. Ozonation in different concentrations of ozone gas

Concentration of ozone strongly affects how fast the oxidation is. The degradation of MB solution using the sea water is measured by varying the ozone concentration as plotted in Fig. 5(a). It is noted here the ozone concentration refers to the amount of ozone in the pumping gas, not directly the concentration of dissolved ozone in water samples. This is because it is more convenient to measure and is thus used as a control parameter. The amount of dissolved ozone can be calculated based on the above-mentioned relationship $H = H^{cp} \times RT$.

In Fig. 5(a), the vertical axis is the degradation exponent DE as defined by

$$DE = \ln\left(\frac{C_o}{C}\right) \quad (8)$$

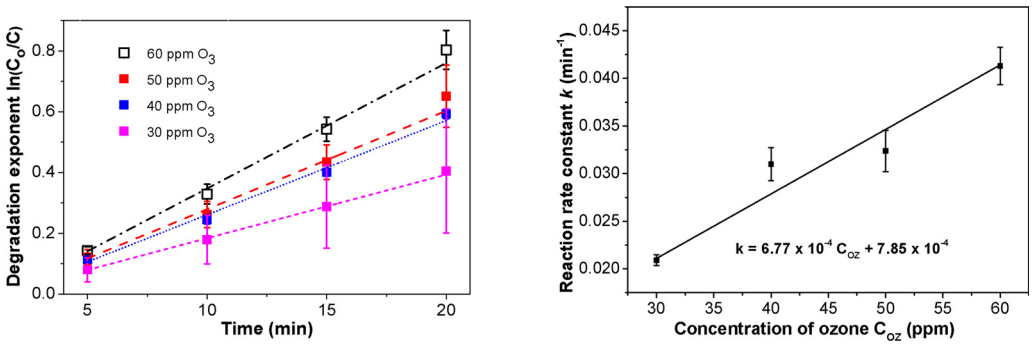

Fig. 5. Measured performance of only the ozonation in sea water. (a) Degradation of methylene blue under different ozone concentrations in the pumping gas. (b) Dependence of the reaction rate constant k on the ozone concentration C_{oz}, which roughly follows a linear relationship $k = 6.77 \times 10^{-4} C_{oz} + 7.85 \times 10^{-4}$ min^{-1}.

here ln denotes natural logarithm, C_o and C are the initial concentration and the resulted concentration of MB solution, respectively. For the first-order reaction, it should have

$$C = C_o \exp(-kt) \tag{9}$$

here k is the reaction rate constant and t is the reaction time. For the first-order reaction, it has

$$DE = kt \tag{10}$$

Therefore, the value of DE is linear to t and the slope of the curve DE versus t is just k.

One can see from Fig. 5(a) that an increase of ozone concentration leads to a higher DE. If we look at the error bars (a result of 5 repeated tests), we can see the error range decreases with higher ozone concentration, indicating better repeatability. This might be because ozone is an unstable gas. A higher concentration of ozone could reduce the uncertainty. For safety reason, 0.01–8 ppm of dissolved ozone is the maximum limit to human. Here 60 ppm of ozone in gas phase corresponds to 0.026 ppm of dissolved ozone in liquid phase. Therefore, if this study uses maximum 60-ppm ozone in gas, it is far safer than the previous studies that often used more than 5000-ppm ozone for the water treatment. In addition, the use of low ozone concentration helps reduce the cost and is thus favorable for practical applications.

Based on above discussion, the slope of degradation exponent denotes the reaction rate constant. We calculate the slopes of curves in Fig. 5(a) and plot in Fig. 5(b) the relationship with the ozone concentration C_{oz} in the pumping gas. It follows roughly a linear relationship $k = 6.77 \times 10^{-4} C_{oz} + 7.85 \times 10^{-4}$ min^{-1}, here C_{oz} is in the unit of ppm.

4.3. Photocatalytic ozonation: degradation versus ozone concentration

The efficiency of PCO in sea water have been tested under different concentrations of ozone. The results are plotted in Fig. 6(a). The photocatalysis without ozone (i.e., 0 ppm ozone) is also plotted as a reference. For a given ozone concentration, the degradation exponent increases almost linearly with t. And an increase of ozone concentration results in a higher degradation exponent. Similarly, we plot the slopes of the curves of Fig. 6(a) as a function of the ozone concentration in pumping gas. The result is plotted in Fig. 6(b), which shows clearly a good linearity. The expression is $k = 8.00 \times 10^{-4} C_{oz} + 1.78 \times 10^{-2}$ min^{-1}. When we compare Fig. 5(b) (for only the ozonation) and Fig. 6(b) (for the PCO), we can see that (i) the data points in Fig. 6(b) have smaller error ranges, showing the PCO in sea water has better stability and repeatability; (ii) Fig. 6(b) has better linearity, showing that the PCO has more controllability; and (iii) The PCO is more effective than the ozonation in the decontamination of seawater. In Fig. 5(b), it has $k = 6.77 \times 10^{-4} C_{oz} + 7.85 \times 10^{-4}$ min^{-1}, whereas in Fig. 6(b), it has $k = 8.00 \times 10^{-4} C_{oz} + 1.78 \times 10^{-2}$ min^{-1}. The PCO has the proportional coefficient 8.00×10^{-4} min$^{-1}\cdot$ ppm^{-1}, larger than the value 6.77×10^{-4} min$^{-1}\cdot$ ppm^{-1} of the ozonation. Therefore, the reaction rate constant of PCO increases more rapidly with the ozone concentration than that of only the ozonation. More importantly, the constant term of k factor for the PCO is 1.78×10^{-2} min^{-1}, about 23 times of the constant term 7.85×10^{-4} min^{-1} for the ozonation. These well show that the PCO is better than only the ozonation, which can be regarded as one of the benefits of using the PCO for the decontamination of sea water.

4.4. Photocatalytic ozonation: synergistic effect of photocatalytic ozonation

As stated above, both the photocatalysis and the ozonation play

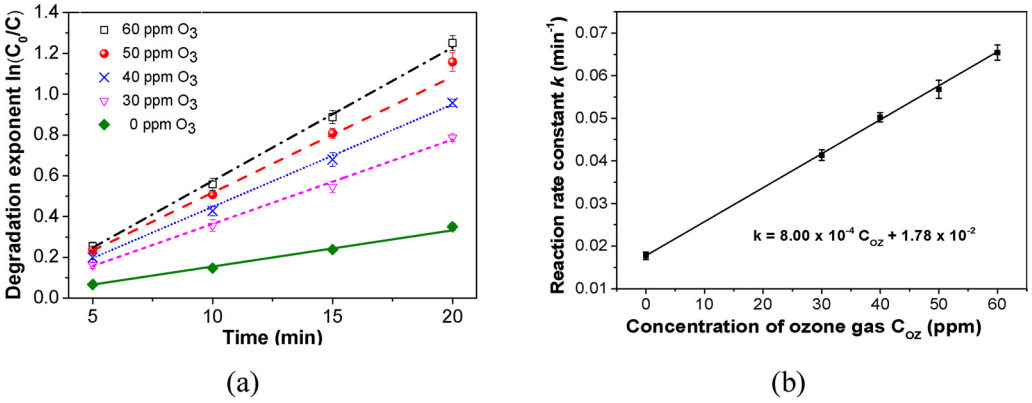

Fig. 6. Measured performance of the photocatalytic ozonation in sea water. (a) Degradation of methylene blue under different ozone concentrations in the pumping gas, in which 0 ppm denotes no ozone and thus the process is only the photocatalysis. (b) Dependence of the reaction rate constant k on the ozone concentration C_{oz}, which closely follows a linear relationship $k = 8.00 \times 10^{-4} C_{oz} + 1.78 \times 10^{-2}$ min^{-1}, when the concentration of ozone gas is low.

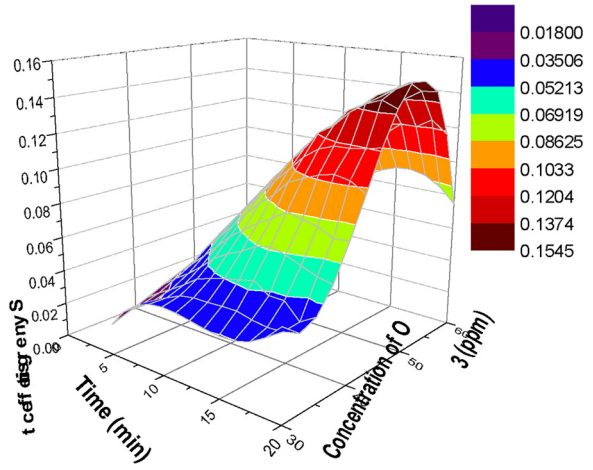

Fig. 7. Synergistic effect of the photocatalytic ozonation in sea water. The synergistic effect is always positive and reaches its maximum when the ozone concentration in the pumping gas is 50 ppm.

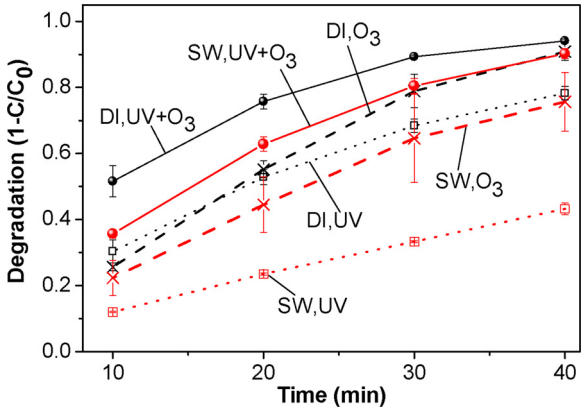

Fig. 8. Comparison of the degradations of methylene blue in fresh water (i.e., DI water) and sea water by the photocatalysis, the ozonation and the photocatalytic ozonation. Under the same condition, the fresh water always shows higher degradation efficiency than the sea water. Labels: SW for sea water, UV for photocatalysis, O_3 for ozonation, and UV + O_3 for photocatalytic ozonation.

roles in the PCO degradation. However, the PCO efficiency is not simply a summation of the photocatalytic efficiency and the ozonation efficiency. Instead, the PCO efficiency could be higher than the summation of the latter two due to the synergistic effect of photocatalysis and ozonation. To quantify the synergistic effect, we can define a parameter S by

$$S = \ln\left(\frac{C_o}{C_{pco}}\right) - \ln\left(\frac{C_o}{C_{pc}}\right) - \ln\left(\frac{C_o}{C_{oz}}\right) = \ln\left(\frac{C_{pc}C_{oz}}{C_o C_{pco}}\right) \tag{11}$$

where C_{pco}, C_{pc}, C_{oz} are the remained MB concentrations of the PCO, the photocatalysis and the ozonation, respectively, all at time *t*. This definition is based on Eq. (9), here the terms $\ln(C_o/C_{pco})$, $\ln(C_o/C_{pc})$ and $\ln(C_o/C_{oz})$ represents the reaction rate constants of the PCO, the photocatalysis and the ozonation, respectively.

Based on the data in Figs. 4 and 5, the synergistic effect of PCO can be calculated. The results are shown by a 3D plot in Fig. 7 as the functions of the time and the ozone concentration. For a fixed ozone concentration, the synergistic effect increases with time and then tends to saturate. At a fixed time, the synergistic effect first goes up when the ozone concentration in gas is increased from 30 ppm to 50 ppm; it reaches the maximum at 50 ppm and then goes down at even higher ozone concentration. In this study, 50 ppm is found to be the optimal condition for the synergistic effect of PCO in sea water.

4.5. Photocatalytic ozonation: comparison of degradations in fresh water and sea water

Using the optimal concentration of ozone, more thorough degradations of MB in the fresh water (i.e., DI water) and the sea water have been conducted to compare only the photocatalysis, only the ozonation and the PCO effect. The results are plotted and compared in Fig. 8. The vertical axis is the degradation, which is defined as

$$Degradation = 1 - \frac{C}{C_o} \tag{12}$$

In the initial state, the degradation is 0; and when the MB is completely degraded, the degradation becomes 1. Several findings can be observed in Fig. 8. (i) The degradation tends to saturate at high level (degradation > 0.5), this is more obvious when the degradation approaches 1. This is a common phenomenon in oxidative degradation. (ii) The fresh water has always higher degradation than the sea water, regardless of photocatalysis, ozonation or PCO. This matches the above prediction (in the mechanism part) that the sea water has weaker oxidation power since the Cl^- ions convert highly oxidative radicals like *OH and O_3^- into relatively weak radicals like OCl* and $*ClO_3$. (iii) The fresh water has smaller error ranges than the sea water. Again, this is because the salt ions disturb the oxidation process and causes uncertainty.

4.6. Photocatalytic ozonation: comparison of synergistic effects in fresh water and sea water

As discussed above, the fresh water has always higher degradation than the sea water. Consequently, the fresh water may have smaller synergistic effect than the sea water. Fig. 9 compares the synergistic effects of the PCO in fresh water and sea water under 50 ppm ozone. In sea water, the synergistic effect increases slightly with the lapse of time. Oppositely, the synergistic effect of fresh water becomes negatively and further drops quickly with time. The reason might be that 50-ppm ozone is not the optimal condition for the PCO in fresh water. Instead, it is too high to make the direct oxidation reaction of ozone dominant, and thus the high ozone concentration would reduce the synergistic effect to negative.

4.7. Photocatalytic ozonation: influence of salt concentration on degradation efficiency

To examine the influence of salinity, the PCO experiments are conducted using the sea water with different salt concentrations. The

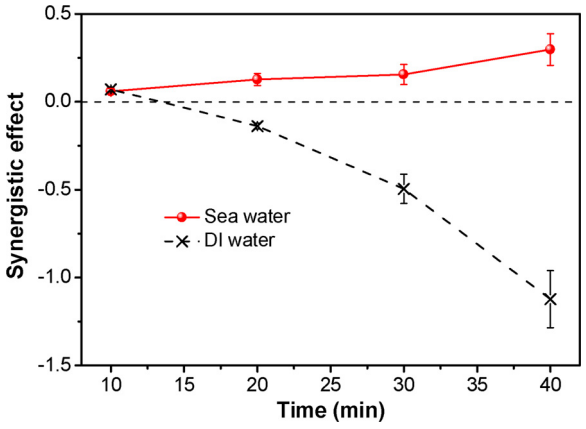

Fig. 9. Comparison of the synergistic effects in fresh water (i.e., DI water) and sea water when the pumping gas has the ozone concentration of 50 ppm, which is optimal for the photocatalytic ozonation of sea water. Here the synergistic effect is given by Eq. (11).

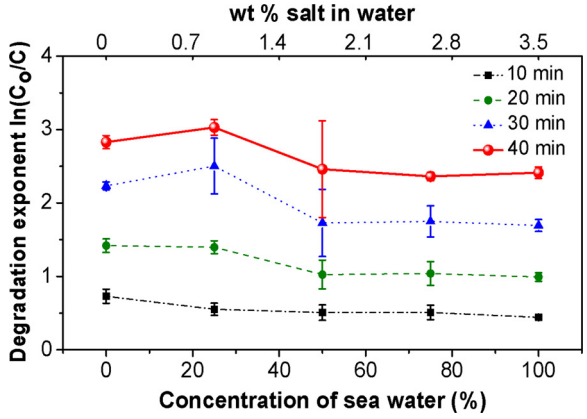

Fig. 10. Degradation performance in sea water with different salt concentrations. The upper x axis is the weight percentage of salt in water, whereas the lower x axis is the relative concentration to the standard 3.5 wt% sea water.

Table 3
Functional effects in different treatments and their influences on the synergistic effect.

	Photolysis effect	Photocatalytic effect	Ozonation effect
Photocatalysis process	Yes	Yes	—
Ozone process	—	—	Yes
PCO process	Yes	Yes	Yes
Synergistic effect	Removed	Included	Included

results are plotted in Fig. 10. It shows clearly that a lower salinity leads to a higher degradation efficiency, but the difference is not that large. At the sampling times of 20 s, 30 s and 40 s, the highest degradation occurs at the 25 % concentration (corresponding to 0.875 wt%), not at 0% (i.e., fresh water). As stated above, the salt ions increase the conversion of dissolved ozone, but they convert the highly-oxidative ions (e.g., *OH) into relatively weak ions (e.g., Cl*, OCl*) and thus lower the oxidizing power. 25 % concentration of sea water may make a good trade-off between these two factors and thus results in the optimal degradation.

4.8. Photocatalytic ozonation: influence of UV photolytic effect on synergistic effect

UV photolysis of MB dyes may affect the photocatalysis treatment and the PCO treatment. Table 3 lists the major effects in each treatment. Fortunately, the definition of synergistic effect in Eq. (11) uses the PCO to deduct the photocatalysis, which makes sure that the contribution of UV photolytic effect is already removed.

4.9. Comparison of this work with previous studies

This work is the first attempt of the PCO treatment of sea water, and has demonstrated superior performance as compared to the reported studies of the PCO treatment of fresh water or gas. For instance, Hur et al. reported a 2.3-fold enhancement in the PCO treatment of fresh water [54]; Yu and Lee presented a 2.6-fold enhancement in the PCO removal of toluene gas [47]. In contrast, this work has obtained a 23-fold enhancement. In term of the enhancement factor, our work is about 10 times of the previous studies. This is really impressive. Of course, it is not very meaningful to directly compare the enhancement factors. As stated above, in sea water the ozonation itself has low efficiency, providing a low reference. Thanks to the synergistic effect of the PC and the ozonation, the PCO treatment can decompose and mineralize the organic contaminants in sea water with high efficiency.

5. Conclusions

The degradation performance of photocatalytic ozonation in sea water has been studied in various aspects. And different properties of sea water and fresh water have also been examined as well when subject to photocatalysis and ozonation. The experimental results well show that the photocatalytic ozonation is efficient for sea water decontamination and enjoys a positive synergistic effect, which is maximized when the pumping gas has the ozone concentration of 50 ppm. This helps reduce the ozone consumption and is favorable for further practical applications in the future.

Author contributions

All authors have read and agreed to the published version of the manuscript.

Funding

This research is supported by Research Grants Council (RGC) of Hong Kong (152184/15E, 152127/17E, 152126/18E and 152219/19E) and The Hong Kong Polytechnic University (1-ZE14, 1-ZE27 and 1-ZVGH).

CRediT authorship contribution statement

Chi Chung Tsoi: Data curation, Formal analysis, Methodology, Writing - review & editing. **Xiaowen Huang:** Formal analysis, Methodology. **Polly H.M. Leung:** Conceptualization, Resources. **Ning Wang:** Formal analysis. **Weixing Yu:** Resources. **Xuming Zhang:** Conceptualization, Investigation, Project administration, Supervision, Writing - review & editing.

Declaration of Competing Interest

The authors declare no conflict of interest. The funders had no role in the design of the study; in the collection, analyses, or interpretation of data; in the writing of the manuscript, or in the decision to publish the results.

Acknowledgments

The technical assistance and facility support from Materials Research Centre, and University Research Facility in Material Characterization and Device Fabrication of The Hong Kong Polytechnic University are greatly appreciated.

References

[1] D. Rubio, J.F. Casanueva, E. Nebot, Improving UV seawater disinfection with immobilized TiO2: Study of the viability of photocatalysis (UV254/TiO2) as seawater disinfection technology, J. Photochem. Photobiol. A Chem. 271 (2013) 16–23, https://doi.org/10.1016/j.jphotochem.2013.08.002.
[2] B. Kasprzyk-hordern, M. Ziółek, J. Nawrocki, Catalytic ozonation and methods of enhancing molecular ozone reactions in water treatment, Appl. Catal. B Environ. 46 (2003) 639–669, https://doi.org/10.1016/S0926-3373(03)00326-6.
[3] S. Malato, P. Fernández-Ibáñez, M.I. Maldonado, J. Blanco, W. Gernjak, Decontamination and disinfection of water by solar photocatalysis: recent overview and trends, Catal. Today 147 (2009) 1–59, https://doi.org/10.1016/j.cattod.2009.06.018.
[4] J. Peral, X. Domènech, D.F. Ollis, Heterogeneous photocatalysis for purification, decontamination and deodorization of air, J. Chem. Technol. Biotechnol. 70 (1997) 117–140, https://doi.org/10.1002/(SICI)1097-4660(199710)70:2<117::AID-JCTB746>3.0.CO,2-F.
[5] Y. Tang, C. Hu, Y. Wang, Recent advances in mechanisms and kinetics of TiO2 photocatalysis, Prog. Chem. 14 (2002) 192–199 DocID:1005281x-200205-14-3-192-199-a.
[6] K. Hashimoto, H. Irie, A. Fujishima, TiO2 Photocatalysis: a historical overview and future prospects kazuhito, Jpn. J. Appl. Phys. 44 (2005) 8269–8285, https://doi.org/10.1143/JJAP.44.8269.

[7] F.E. Osterloh, Inorganic materials as catalysts for photoelectrochemical splitting of water, Chem. Mater. 20 (2008) 35, https://doi.org/10.1021/cm7024203.

[8] Y. Nakamura, F. Kobayashi, M. Daidai, A. Kurosumi, Purification of seawater contaminated with undegradable aromatic ring compounds using ozonolysis followed by titanium dioxide treatment, Mar. Pollut. Bull. 57 (2008) 53–58, https://doi.org/10.1016/j.marpolbul.2007.10.003.

[9] R.M. Brookman, R. Lamsal, G.A. Gagnon, Comparing the formation of bromate and bromoform due to ozonation and UV-TiO2 oxidation in seawater, J. Adv. Oxid. Technol. 14 (2011) 23–30, https://doi.org/10.1515/jaots-2011-0103.

[10] L. Wenhua, L. Hong, C. Sao'an, Z. Jianqing, C. Chunan, Kinetics of photocatalytic degradation of aniline in water over TiO2 supported on porous nickel, J. Photochem. Photobiol. A Chem. 131 (2000) 125–132, https://doi.org/10.1016/S1010-6030(99)00232-4.

[11] C.C. Wong, W. Chu, The direct photolysis and photocatalytic degradation of alachlor at different TiO2 and UV sources, Chemosphere 50 (2003) 981–987, https://doi.org/10.1016/S0045-6535(02)00640-9.

[12] K. Wang, J. Zhang, L. Lou, S. Yang, Y. Chen, UV or visible light induced photodegradation of AO7 on TiO2 particles: The influence of inorganic anions, J. Photochem. Photobiol. A Chem. 165 (2004) 201–207, https://doi.org/10.1016/j.jphotochem.2004.03.025.

[13] C. Guillard, et al., Influence of chemical structure of dyes, of pH and of inorganic salts on their photocatalytic degradation by TiO2 comparison of the efficiency of powder and supported TiO2, J. Photochem. Photobiol. A Chem. 158 (2003) 27–36, https://doi.org/10.1016/S1010-6030(03)00016-9.

[14] N. Wang, F.R. Tan, C.C. Tsoi, X.M. Zhang, Photoelectrocatalytic microreactor for seawater decontamination with negligible chlorine generation, Microsyst. Technol. 23 (2017) 4495–4500.

[15] J.C. Perrins, W.J. Cooper, J.H. Leeuwen, R.P. Van; Herwig, Ozonation of seawater from different locations : formation and decay of total residual oxidant — implications for ballast water treatment, Mar. Pollut. Bull. 52 (2006) 1023–1033, https://doi.org/10.1016/j.marpolbul.2006.01.007.

[16] Y. Penru, et al., Disinfection of seawater: application of UV and ozone, Ozone Sci. Eng. 35 (2017) 63–70, https://doi.org/10.1080/01919512.2012.722050.

[17] T.E. Agustina, H.M. Ang, V.K. Vareek, A review of synergistic effect of photocatalysis and ozonation on wastewater treatment, J. Photochem. Photobiol. C Photochem. Rev. 6 (2005) 264–273, https://doi.org/10.1016/j.jphotochemrev.2005.12.003.

[18] M. Jacek, Methods for measuring ozone concentration in ozone-treated water, Prz. Elektrotechniczny 88 (2012) 253–255, https://doi.org/10.1016/j.aquaeng.2005.02.002.

[19] D. Bahnemann, Photocatalytic water treatment: solar energy applications, Sol. Energy 77 (2004) 445–459, https://doi.org/10.1016/j.solener.2004.03.031.

[20] M.N. Chong, B. Jin, C.W.K. Chow, C. Saint, Recent developments in photocatalytic water treatment technology: a review, Water Res. 44 (2010) 2997–3027, https://doi.org/10.1016/j.watres.2010.02.039.

[21] S. Banerjee, P. Benjwal, M. Singh, K.K. Kar, Graphene oxide (rGO)-metal oxide (TiO2/Fe3O4) based nanocomposites for the removal of methylene blue, Appl. Surf. Sci. 439 (2018) 560–568, https://doi.org/10.1016/j.apsusc.2018.01.085.

[22] P. Benjwal, B. De, K.K. Kar, 1-D and 2-D Morphology of metal cation co-doped (Zn, Mn) TiO2 and investigation of their photocatalytic activity, Appl. Surf. Sci. 427 (2018) 262–272, https://doi.org/10.1016/j.apsusc.2017.08.226.

[23] P. Benjwal, R. Sharma, K.K. Kar, Effects of surface microstructure and chemical state of featherfiber-derived multidoped carbon fibers on the adsorption of organic water pollutants, Mater. Des. 110 (2016) 762–774, https://doi.org/10.1016/j.matdes.2016.08.030.

[24] P. Benjwal, M. Kumar, P. Chamoli, K.K. Kar, Enhanced photocatalytic degradation of methylene blue and adsorption of arsenic(iii) by reduced graphene oxide (rGO)–metal oxide (TiO2/Fe3O4) based nanocomposites, RSC Adv. (5) (2015) 73249–73260, https://doi.org/10.1039/C5RA13689J.

[25] P. Benjwal, K.K. Kar, Removal of methylene blue from wastewater under a low power irradiation source by Zn, Mn co-doped TiO2 photocatalysts, RSC Adv. 5 (2015) 98166–98176, https://doi.org/10.1039/C5RA19353B.

[26] P. Benjwal, K.K. Kar, One-step synthesis of Zn doped titania nanotubes and investigation of their visible photocatalytic activity, Mater. Chem. Phys. 160 (15 June) (2015) 279–288.

[27] P. Benjwal, K.K. Kar, Simultaneous photocatalysis and adsorption based removal of inorganic and organic impurities from water by titania/activated carbon/carbonized epoxy nanocomposite, J. Environ. Chem. Eng. 3 (2015) 2076–2083, https://doi.org/10.1016/j.jece.2015.07.009.

[28] N. Wang, F. Tan, L. Wan, M. Wu, X. Zhang, Microfluidic reactors for visible-light photocatalytic water purification assisted with thermolysis, Biomicrofluidics 8 (2014) 1074–1082, https://doi.org/10.1063/1.4899883.

[29] D. Alibegic, S. Tsuneda, A. Hirata, Oxidation of tetrachloroethylene in a bubble column photochemical reactor applying the UV/H2O2 technique, Can. J. Chem. Eng. 81 (2003) 733–740, https://doi.org/10.1002/cjce.5450810353.

[30] S. Gautam, S.P. Kamble, S.B. Sawant, V.G. Pangarkar, Photocatalytic degradation of 4-nitroaniline using solar and artificial UV radiation, Chem. Eng. J. 110 (2005) 129–137, https://doi.org/10.1016/j.cej.2005.03.021.

[31] P.K. Surolia, R.J. Tayade, R.V. Jasra, Effect of anions on the photocatalytic activity of Fe (III) salts impregnated TiO 2, Society 46 (2007) 6196–6203, https://doi.org/10.1021/ie0702678.

[32] M. Muruganandham, M. Swaminathan, Solar photocatalytic degradation of a reactive azo dye in TiO 2-suspension, Sol. Energy Mater. Sol. Cells 81 (2004) 439–457, https://doi.org/10.1016/j.solmat.2003.11.022.

[33] J. Kiwi, A. Lopez, V. Nadtochenko, Mechanism and kinetics of the OH-radical intervention during Fenton oxidation in the presence of a significant amount of radical scavenger (Cl-), Environ. Sci. Technol. 34 (2000) 2162–2168, https://doi.org/10.1021/es991406i.

[34] C. Guillard, E. Puzenat, H. Lachheb, A. Houas, J.-M. Herrmann, Why inorganic salts decrease the TiO2 photocatalytic efficiency, Int. J. Photoenergy 7 (2005) 1–9, https://doi.org/10.1155/S1110662X05000012.

[35] A. Sclafani, L. Palmisano, E. Davì, Photocatalytic degradaton of phenol in aqueous polycrystalline TiO2 dispersions: the influence of Fe3+, Fe2+ and Ag+ on the reaction rate, J. Photochem. Photobiol. A Chem. 56 (1991) 113–123, https://doi.org/10.1016/1010-6030(91)80011-6.

[36] M. Fujuhira, Y. Satoh, T. Sa, Heterogeneous photocatalytic reactions on semiconductor materials. III. Effect of pH and Cu2+ on the photo-fenton type reaction, Bull. Chem. Soc. Jpn. 55 (1982) 666–671, https://doi.org/10.1246/bcsj.55.666.

[37] M. Abdullah, G.K.-C. Low, R.W. Matthews, Effects of common inorganic anions on rates of photocatalytic oxidation of organic carbon over illuminated titanium dioxide, J. Phys. Chem 94 (1990) 6820–6825, https://doi.org/10.1021/j100380a051.

[38] C. Kormann, D.W. Bahnemann, M.R. Hoffmann, Photolysis of chloroform and other organic molecules in aqueous TiO, suspensions, Environ. Sci. Technol. 25 (1991) 494–500, https://doi.org/10.1021/es00015a018.

[39] D.F. Ollis, C.Y. Hsiao, L. Budiman, C.L. Lee, Heterogeneous photoassisted catalysis: Conversions of perchloroethylene, dichloroethane, chloroacetic acids, and chlorobenzenes, J. Catal. 88 (1984) 89–96, https://doi.org/10.1016/0021-9517(84)90053-8.

[40] N. Wang, X.M. Zhang, Y. Wang, W.X. Yu, H.L.W. Chan, Microfluidic reactors for photocatalytic water purification, Lab Chip 14 (2014) 1074–1082, https://doi.org/10.1039/C3LC51233A.

[41] L.J. Jack, Criegee mechanism of ozonolysis, Name Reactions: A Collection of Detailed Mechanisms and Synthetic Applications, 4th, ed., Springer Berlin Heidelberg, Berlin, German, 2009, p. 161.

[42] R. Criegee, Mechanism of ozonolysis, Angew. Chem. Int. Ed. English 14 (1975) 745–752, https://doi.org/10.1002/anie.197507451.

[43] U. Von Gunten, Ozonation of drinking water: Part I. Oxidation kinetics and product formation, Water Res. 37 (2003) 1443–1467, https://doi.org/10.1016/S0043-1354(02)00457-8.

[44] L.R.B. Yeatts, H. Taube, The kinetics of the reaction of ozone and chloride ion in acid aqueous solution, J. Am. Chem. Soc. 71 (1949) 4100–4105, https://doi.org/10.1021/ja01180a063.

[45] W.R. Haag, On the disappearance of chlorine in sea-water, Water Res. 15 (1981) 937–940, https://doi.org/10.1016/0043-1354(81)90151-2.

[46] L. Sánchez, J. Peral, X. Domènech, Aniline degradation by combined photocatalysis and ozonation, Appl. Catal. B Environ. 19 (1998) 59–65, https://doi.org/10.1016/S0926-3373(98)00058-7.

[47] Yu Kuo-Pin, Grace W.M. Lee, Decomposition of gas-phase toluene by the combination of ozone and photocatalytic oxidation process (TiO2/UV, TiO2/UV/O3, and UV/O3), Appl. Catal. B Environ. 75 (1–2) (2007) 29–38, https://doi.org/10.1016/j.apcatb.2007.03.006.

[48] R. Battino, T.R. Rettich, T. Tominaga, The solubility of nitrogen and air in liquids, J. Phys. Chem. Ref. Data 13 (1984) 563–600, https://doi.org/10.1063/1.555713.

[49] S. Morooka, K. Ikemizu, H. Kamano, Y. Kato, Ozonation rate of water-soluble chelates and related compounds, J. Chem. Eng. Jpn. 19 (1986) 294–299 https://www.jstage.jst.go.jp/article/jcej1968/19/4/19_4_294/_pdf.

[50] J.J. Wu, S.J. Masten, Mass transfer of ozone in semibatch stirred reactor, J. Environ. Eng. 127 (2001) 1089–1099, https://doi.org/10.1061/(ASCE)0733-9372(2001)127:12(1089).

[51] F. Lynn, C. Kosak, R. Oeorge, Helz solubility of ozone in aqueous solutions of 0-0.6M ionic strength at 5-30C, Environ. Scl. Technol 17 (1983) 145–149, https://doi.org/10.1021/es00109a005.

[52] V. Caprio, A. Insola, P.G. Lignola, G. Volpicelli, A new attempt for the evaluation of the absorption constant of ozone in water, Chem. Engng Sci. 37 (1982) 122–123, https://doi.org/10.1016/0009-2509(82)80076-6.

[53] J.L. Sotelo, F.J. Beltrán, M. González, J. Domínguez, Effect of high salt concentrations on ozone decomposition in water, J. Environ. Sci. Heal. Part A Environ. Sci. Eng. 24 (1989) 823–842, https://doi.org/10.1080/10934528909375518.

[54] J.S. Hur, S.O. Oh, K.M. Lim, J.S. Jung, J.W. Kim, Y.J. Koh, Novel effects of TiO2 photocatalytic ozonation on control of postharvest fungal spoilage of kiwifruit, Postharvest Biol. Technol. 35 (2005) 109–113.